

See discussions, stats, and author profiles for this publication at: <https://www.researchgate.net/publication/12809744>

Electrical Equivalence of Electrospray Ionization with Conducting and Nonconducting Needles

ARTICLE in ANALYTICAL CHEMISTRY · OCTOBER 1999

Impact Factor: 5.64 · DOI: 10.1021/ac9902244 · Source: PubMed

CITATIONS

51

READS

39

2 AUTHORS:



[George Jackson](#)

Purdue University

45 PUBLICATIONS 1,774 CITATIONS

SEE PROFILE



[Chris Enke](#)

University of New Mexico

198 PUBLICATIONS 4,582 CITATIONS

SEE PROFILE

Electrical Equivalence of Electrospray Ionization with Conducting and Nonconducting Needles

George S. Jackson and Christie G. Enke*

Department of Chemistry, The University of New Mexico, Albuquerque, New Mexico 87131

An electrical equivalent circuit is derived for the electrospray process. It is a series circuit which consists of the power supply, the electrochemical contact to the solution, the solution resistance (R_s), a constant-current regulator which represents the processes of charge separation and charge transport in the gap between the spray needle aperture and the counter electrode, and charge neutralization at the counter electrode. A current i , established by the constant-current regulator flows throughout the entire circuit. Current–voltage curves are developed for each element in the circuit. From these it is shown that in the case where R_s is negligible (the power supply is connected directly to a conducting needle) the shape of the current–voltage curve is dictated by the constant-current regulator established by the charge separation process, the gap, and the counter electrode. The solution resistance may be significant if a nonconducting needle is used so that the electrochemical contact to the solution is remote from the tip. Experiments with a nonconducting spray needle quantify the effect of the solution resistance on the current–voltage curve. Subtracting the iR_s voltage from V_{app} (power supply voltage) yields the current–voltage curve for the constant-current regulator. When iR_s drop is a significant fraction of V_{app} , the current–voltage curve of the constant-current regulator is changed substantially from the case when the solution resistance is negligible.

Electrospray ionization is clearly an electrical phenomenon. To aid the understanding of electrical phenomena, an equivalent circuit is often drawn. In an equivalent circuit, electrical components of known properties are used to simulate the behavior of the actual circuit. In the equivalent circuit, one chooses components that have a current–voltage behavior similar to that of the individual elements in the actual circuit. In this paper, we have analyzed each of the elements in the electrospray circuit with respect to its current–voltage curve so that an appropriate equivalent circuit can be drawn. The achievement of a useful equivalent circuit serves the purpose of separating the electrical effects of the various circuit elements so that they may be studied and understood individually. This is particularly advantageous in a system with so many interactive elements as electrospray ionization.

The accepted functional schematic for the electrospray ionization process is shown in Figure 1.^{1,2} The voltage from the power supply is connected to a metal contact through which the analyte solution flows. The metal contact may be the metallic electrospray needle itself or a metallic union that joins the needle to the capillary tubing that supplies the analyte. The connection between the metal and the analytical solution is essentially electrochemical.^{1,3–6} The analytical solution issues from the spray tip in the form of charged droplets. The droplets have the same charge sign as the pole of the power supply that is connected to the electrochemical contact. The charged droplets are attracted across an air gap to the counter electrode where many of the droplets are neutralized, and that portion of the current (i_{ce} in Figure 1) is returned to the power supply. The connection between the counter electrode and the other pole of the power supply completes the circuit. A small orifice in the counter electrode allows some of the ions from the solution to enter the vacuum chamber of the mass spectrometer for mass analysis. The fraction of charge that enters the orifice is also eventually neutralized, and that portion of the current (i_{ms} in Figure 1) is returned to the power supply. Since all of the charge neutralization events occur in parallel, we will consider them as one event for the rest of the discussion, and they will be represented by one symbol in the final equivalent circuit. With this minor simplification, all the elements and processes in the electrospray circuit are in series, as shown, so that the total current (i in Figure 1) that flows in this circuit is everywhere the same.

A circuit that separates the several processes of electrospray ionization is shown in Figure 2. Most of the processes are shown as functional blocks rather than circuit components, as it is the goal of this paper to identify the electrical nature of each process by the study of its current–voltage curve. The processes in Figure 2 can be related to the circuit elements in Figure 1 as follows. The electrochemical contact occurs between the metal to which the power supply is connected and the solution in that region of the metal/solution contact closest to the electrospray tip.⁷ If the connection is to a metallic union and a nonmetallic glass capillary

- (1) Blades, A. T.; Ikononou, M. G.; Kebabian, P. *Anal. Chem.* **1991**, *63*, 2109–2114.
- (2) Kebabian, P.; Tang, L. *Anal. Chem.* **1993**, *65*, 972A–985A.
- (3) Van Berkel, G. J.; Zhou, F. *Anal. Chem.* **1995**, *67*, 2916–2923.
- (4) Van Berkel, G. J. In *Electrospray Ionization Mass Spectrometry*; Cole, R. B., Ed.; John Wiley & Sons: New York, 1997; pp 65–105.
- (5) Simons, D. S.; Colby, B. N.; Evans, C. A. *Int. J. Mass Spectrom. Ion Phys.* **1974**, *15*, 291–302.
- (6) Van Berkel, G. J.; McLuckey, S. A.; Glish, G. L. *Anal. Chem.* **1992**, *64*, 1586–1593.
- (7) Enke, C. G. *Anal. Chem.* **1997**, *69*, 4885–4893.

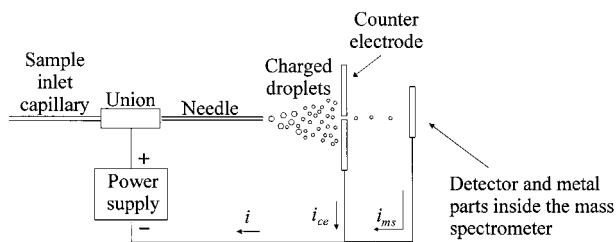


Figure 1. Accepted functional schematic for the ESI process.

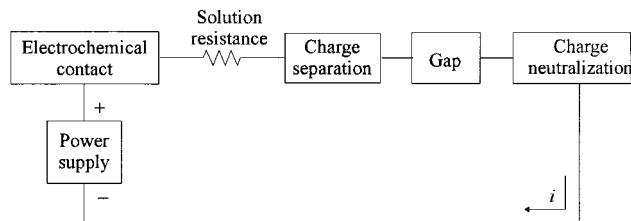


Figure 2. Circuit for ESI with many of the processes shown as functional blocks.

is used as the spray needle,⁸ there may be some solution resistance between the electrochemical contact and the spray tip.⁹ At the needle tip, charge separation occurs as a result of the high electric field that exists between the tip and the counter electrode. The charge separation is in the formation of the charged droplets that emanate from the tip. The charged droplets are then attracted across the air gap between the tip and the counter electrode. All of the charge that is separated at the tip is neutralized at the counter electrode or inside the mass spectrometer and returned to the power supply. Another characteristic of a series circuit is that the sum of voltage drops across all the processes shown must equal the voltage applied by the power supply. If the current-voltage behavior of each of the processes is characterized, then the degree to which the several processes are independent or interdependent can be more readily understood.

THEORY

In this section, we will look at the way in which the current-voltage curve has been or could be determined for each process or circuit element shown in Figure 2 and assign, where possible, suitable equivalent circuit components. In the first instance, we will assume that a metal needle is used so that the solution resistance is zero or negligible. This analysis is done for ESI in the positive-ion mode.

The Power Supply. The power supply is presumed to provide a constant voltage regardless of the current required of it (over the reasonable ESI operating range). The electrical equivalent of this is a battery of the set voltage (V_{app}) with an internal resistance of $0\ \Omega$. For this device, the plot of current vs voltage would be a vertical line at V_{app} as shown in Figure 3a. The internal resistance of the power supply is obtained from the differential definition of resistance, i.e., $R = dV/di$. Since the voltage does not change with the amount of current drawn, the resistive component of the power supply is zero. The other important point about the power supply is that its setting determines the total voltage, V_{app} , applied to the

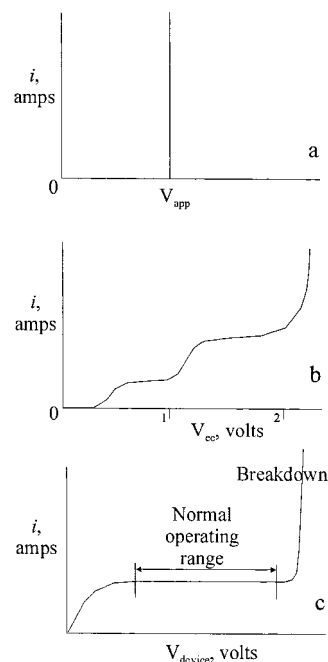


Figure 3. The current-voltage curves for (a) the current vs the power supply voltage (V_{app}), (b) the current vs the electrochemical voltage (V_{ec}), and (c) the current vs V_{device} for a current-limited device.

overall electrospray process. The individual voltages of all the individual ESI processes will sum to equal the voltage V_{app} .

The Electrochemical Contact. Much has been written about the electrochemical nature of the contact between the power supply and the solution that is to be electrosprayed.^{1-4,6,10-15} The entire electrospray process has been likened to an electrochemical cell where the metal-solution contact is the anode (when making positive ions) and the counter electrode, where the charge neutralization occurs, is the cathode. The current-voltage curves of electrochemical processes have been well characterized by the community of electrochemists and applied to the contact process in ESI. The general nature of the electrochemical current-voltage curve is shown in Figure 3b.³ The voltage corresponding to the first rise in current corresponds to the oxidation potential of the most easily oxidizable solution component. Further increases in voltage do not cause this reaction to accelerate, which is why no increase in the current is observed. This is because the reaction is now limited by the rate of diffusion of the oxidizable species to the metal surface.

The second rise in current occurs at the oxidation potential of the second most readily oxidized solution component. The rate of its oxidation may also become diffusion limited. Eventually, if one increases the voltage or current sufficiently, one encounters the potential at which the solvent can become oxidized. This oxidation is not diffusion limited, so the current can rise virtually without limit at this voltage.

(8) Emmett, M. R.; Caprioli, R. M. *J. Am. Soc. Mass Spectrom.* **1994**, *5*, 605-613.

(9) Mazereeuw, M.; Hofte, A. J. P.; Tjaden, U. R.; van der Greef, J. *Rapid Commun. Mass Spectrom.* **1997**, *11*, 981-986.

(10) Van Berkel, G. J.; Giles, G. E.; Bullock, J. S., IV; Wendel, M. W.; Gray, L. J. *Proceedings of the 46th ASMS Conference on Mass Spectrometry and Allied Topics*, Orlando, FL, Am. Soc. Mass Spectrom.: Santa Fe, NM, 1998; p 132.

(11) Xiaomong, X.; Nolan, S. P.; Cole, R. B. *Anal. Chem.* **1994**, *66*, 119-125.

(12) McCarley, T. D.; Lufaso, M. W.; Curtin, L. S.; McCarley, R. L. *J. Phys. Chem. B* **1998**, *102*, 10078-10086.

(13) Vandell, V. E.; Limbach, P. A. *J. Mass Spectrom.* **1998**, *33*, 212-220.

(14) Van Berkel, G. J.; Feimeng, Z. *J. Am. Soc. Mass Spectrom.* **1996**, *7*, 157-162.

(15) Van Berkel, G. J. *J. Anal. At. Spectrom.* **1998**, *13*, 603-607.

The view presented above is oversimplified somewhat because the normal electrochemical current–voltage curve shown is that for an electrode of fixed area and for which the charge transfer process is rapid relative to the rate of diffusion. In the case of ESI, the portion of the metal–solution contact area at which the oxidation is occurring may increase back from the area closest to the tip as the current increases.¹⁰ It is also likely that some charge transfer polarization could occur. These distinctions are important for those studying the analytical implications of the electrochemical reactions on the ES-MS experiment (e.g., analyte ionization, solution pH changes, and generation of chemical noise⁴), but it has a very minor impact on the overall electrical behavior of the ESI circuit. The largest imaginable voltage involved in the electrochemical contact is a few volts, while normal power supply voltages are in the thousands of volts.

Included in the actual current–voltage curve for the electrochemical contact will be the resistance involved in transporting the excess counterions produced at the ESI tip back to the point of the electrochemical process or transporting the excess ions to the ESI tip. When metallic or metallized needles are used (or when the contact is made by a thin wire reaching almost to the tip), the iR drop across this resistance will be at most a few volts. When significant, this resistance will cause some positive slope in the portions of the Figure 3b current–voltage curve that are flat and it will increase the voltage V_{cc} required to achieve a given current. If the electrochemical contact is located far from the tip of a nonconducting needle, the solution resistance can have a significant effect.

The equivalent circuit elements for the electrochemical contact are a voltage source (represented as a battery) and a series resistor. The former represents the voltage required by the electrochemical process for the value of the circuit current. From Figure 3b we can see that the value of this voltage increases in steps according to the circuit current. The polarity of the battery will always oppose that of the power supply. The series resistor is the resistance to the movement of the counterion charge from the tip of the needle to the site of the electrochemical oxidation.

The Charge Separation. As clearly demonstrated by several investigators, there is a charge separation step that occurs in the solution at the needle tip.^{16–18} The strong electric field across the gap draws positive ions in the solution to the exposed surface of the solution. Droplets breaking off from the positively charged solution surface retain some of the excess positive charge. These positively charged droplets are now in the gap between the tip and the counter electrode, and charge separation has occurred. The same field that created the charge separation now attracts the droplets to the counter electrode, where they will be neutralized to complete the circuit. Because of the equality of the current everywhere in the circuit, the rate of formation of excess charge in the droplets is exactly equal to the rate of production of excess anionic charge in the solution, which in turn is exactly equal to the required rate of the electrochemical reaction and the current supplied by the power supply.

Many investigators have studied the current–voltage behavior of the ESI process, much of which is due to the charge separation

process.^{16,18–20} They have shown that it is a complex process dependent on the applied voltage, the solution composition, the distance of the tip from the counter electrode, the flow rate of the solution, and the diameter of the tip. Generally, the relationships involved in the ESI process are expressed in terms of the dependency of the circuit current on the other experimental parameters.

One thing is clear. In normal electrospray, it is the rate of the charge separation process that determines the current that flows in the overall circuit and thus through every other component and process. By normal electrospray, we mean the charge separation resulting from the electrostatic spray process and not from corona discharge or other processes resulting from the breakdown of the insulating properties of the air in the gap. Since the charge separation process controls the current in the circuit,³ the appropriate equivalent circuit element is a constant-current regulator. This is shown by a circle with an arrow indicating the direction of the current.

Understanding the charge separation process is important to understanding the overall ESI process. Some of the difficulty in the interpretation of the current–voltage curves obtained for the overall ESI process has been in the uncertainty of how much of the observed effect is due to processes other than the charge separation process. The advantage of being able to separate out the effects of the other processes from the overall effect to better study the charge separation process is one of the principal points of this paper. For this reason, we will delay discussion of the current–voltage curve of the charge separation process until we have concluded our look at the other processes.

The Gap. As discussed above, charged droplets produced by the charge separation process appear in the gap between the tip and the counter electrode. Because of their charge and the presence of the high electric field in this region, the droplets are drawn toward the counter electrode. While in the gap, the droplets are also undergoing evaporation of the solvent. Solvent evaporation cannot affect the total amount of charge produced by the charge separation process. The field strength required to induce the electrostatic spray process is certainly sufficient to attract and collect the entire charge produced by the charge separation process. The current in the gap is due to and controlled by the rate of charge separation at the needle tip. A change in the gap voltage does not change the fraction of the separated charge collected, since it is always unity.

The process involved in the gap of the ESI system is substantially analogous to that of the gap in a phototube, a photodiode, or a flame ionization detector.⁴ In these devices, the process producing the charge separation is distinct from the collection of the separated charge. The photons striking the photocathode (or depletion region) create electrons (or electron–hole pairs) which then, due to the electric field in the device, are *all* collected by the electrode creating the field. The current in the external circuit is then equal to the rate of charge production and collection. In the case of the flame ionization detector, the ion–electron pairs formed by the flame from the analyte are all collected by the electrodes forming the charge collection field in the device. The current–voltage curves for these devices are of

(16) Ikononou, M. G.; Blades, A. T.; Kebarle, P. *Anal. Chem.* **1990**, *62*, 957.

(17) Ikononou, I. G.; Blades, A. T.; Kebarle, P. *Anal. Chem.* **1991**, *63*, 1989–1998.

(18) Pfeiffer, R. J.; Hendricks, C. D. *AIAA J.* **1968**, *6*, 496.

(19) Tang, L.; Kebarle, P. *Anal. Chem.* **1991**, *63*, 2709–2715.

(20) Tang, L.; Kebarle, P. *Anal. Chem.* **1993**, *65*, 3654–3668.

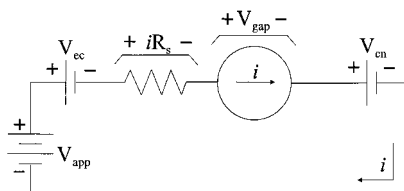


Figure 4. Complete equivalent circuit for ESI in the case of positive-ion generation.

the type shown in Figure 3c. There is a step shape at low applied voltage (collection field strength) where the field is not strong enough to collect all the separated charge before charge recombination can occur. Once a sufficiently strong field has been applied, all the separated charge is collected and the current is limited by the rate of charge separation. The curve in this region is absolutely flat because, in the devices mentioned, the rate of charge separation is a function of the photon flux or the rate of influx of analyte, not the field strength. At a sufficiently high applied field strength, there may be a dielectric breakdown of the medium between the electrodes and a precipitous rise in the current. In this region, the device is no longer functioning for its intended purpose. This would correspond to the discharge region for ESI.

In the case of ESI, there is an opportunity for confusion because the current observed is not independent of the field strength in the gap. However, this dependency is due to the effect of the field strength on the rate of charge separation, not on the effectiveness of the field in collecting all the separated charge. Thus, we believe it is useful to keep these two parts of the process distinct, as they are inherently in the analogous devices. Because the efficiency of charge collection is not a function of the applied field in the normal operating range, a resistive model is not appropriate for the gap. In a resistor, the flux of charge through the resistor is a function of the applied field. In the case of the gap conduction, this is not true. Even if the field strength affects the velocity of the charged particles in the gap, it does not affect the fraction of charges collected. Thus the current is still limited by the rate of charge separation. There is a voltage across the gap, but it is not due to an iR drop caused by the current across it. The voltage is that which is required to provide the field at the tip that leads to the observed rate of charge separation. Fortunately, this same field is high enough to provide for total collection of the separated charge. This voltage is the voltage across the gap and thus is given the symbol V_{gap} .

The Charge Neutralization. Ionic charge crossing the gap hits the counter electrode or enters the orifice to the mass spectrometer. This charge is neutralized by its encounter with metal that is connected to the negative pole of the power supply. The neutralization process for positive ions is an electrochemical reduction.^{1,2,4,21} Very little has been written about the nature of this process.²² Nevertheless, in a manner analogous to the electrochemical contact, only a modest voltage is required for this process to proceed at the rate set by the charge separation. This voltage is symbolized by a battery with polarity opposite to that of the power supply.

The Complete Equivalent Circuit. The resulting complete equivalent circuit is shown in Figure 4 for the case of positive ion generation. It includes all the components discussed above. The constant-current regulator of the electrostatic spray process determines the current i in the circuit. The electrochemical contact and charge neutralization processes are voltages (V_{ec} and V_{cn}) that oppose the applied voltage, V_{app} . The solution resistance, R_s , will result in an iR_s drop also opposing V_{app} . It will only be significant in the case of nonconducting needles. The voltage across the gap, V_{gap} , is then

$$V_{\text{gap}} = V_{\text{app}} - V_{\text{ec}} - iR_s - V_{\text{cn}} \quad (\text{exact}) \quad (1)$$

In the case of a conducting needle, iR_s , V_{ec} , and V_{cn} are all small compared to V_{app} . Therefore, for the conducting needle the following approximation is valid:

$$V_{\text{gap}} \approx V_{\text{app}} \quad (\text{metal needle}) \quad (2)$$

Thus all the current–voltage behavior that has been observed with metal or metal-coated needles has been that of the charge separation process itself. This realization can uncomplicate the interpretation of these data, since none of the other processes can have a significant effect on the overall ESI current–voltage curve. Normal ESI conditions have a current that is on the order of 10^{-7} A and a V_{app} that usually ranges from 2 to 8 kV. Thus, if iR_s is to be large enough for it to be a significant fraction of V_{app} (1 kV or greater), then R_s has to be at least $10^{10} \Omega$ or larger. In the case of a nonconducting needle, the solution resistance can have a significant effect⁹ since it can be $10^{10} \Omega$ or larger, as we will show under Results and Discussion. Also, when iR_s is a significant fraction of V_{app} , eq 1 becomes

$$V_{\text{gap}} \approx V_{\text{app}} - iR_s \quad (\text{nonconducting needle}) \quad (3)$$

EXPERIMENTAL SECTION

The ESI needle assembly consists of a World Precision Instruments (Sarasota, FL) TAURUS-R-X-Y-Z micromanipulator which holds an in-house mount for the ESI needle of choice. The sample is introduced into the ESI needle through a $100 \mu\text{m}$ glass capillary transfer line that is connected to an SGE (Austin, TX) 250 μL gastight syringe using a Harvard Apparatus (South Natick, MA) model 22 syringe pump. The high-voltage power supply is connected directly to the needle. For the nonconducting glass capillary experiments, a 25 or 50 μm i.d. glass capillary is used as the needle. The electrical contact is made through the stainless steel union between the fused-silica capillary transfer line and the glass needle. In some experiments (nonconducting glass capillary needle and conventional ESI configurations), a $5 \times 10^{10} \Omega$ Victoreen (Cleveland, OH) resistor is placed between the high-voltage power supply and the connection to the needle. Unless otherwise noted, the flow rate (Γ) for the 25 and 50 μm glass capillary spray needles is 1 $\mu\text{L}/\text{min}$ and the flow rate for the stainless steel needle ($\sim 250 \mu\text{m}$ i.d.) is 8 $\mu\text{L}/\text{min}$. The flow rate was measured under all of the experimental conditions, and the amount of sample consumed always coincided with the requested flow rate. Furthermore, the whole assembly was analyzed for leaks and none were found. Also, the distance between the spray needle

(21) Charbonier, F.; Nicolas, J. P.; Eveleigh, L.; Hapiot, P.; Pinson, J.; Rolando, C. *C. R. Acad. Sci., Ser. II: Chim.* **1998**, *1*, 449–456.

(22) Lavanant, H.; Virelizier, H.; Hoppilliard, Y. *J. Am. Soc. Mass Spectrom.* **1998**, *9*, 1217–1224.

and the metal plate was 1 mm for the glass spray needles and 3.5 mm for the metal spray needles. Unless otherwise noted, the needle length for all the nonconducting glass capillary glass spray needles was 5 cm. The current was measured with an ammeter that was connected between the spray needle and the power supply. For most of the measurements taken, little variation was observed in the measured current (in fact, it was usually less than 1%). The only conditions under which the measured current was not very stable were those where we were spraying out of a metal needle and the measured current was high (>100 nA). Electrophoretic migration of the charge back toward the syringe pump and ground was ruled out when the ammeter that was connected between the spray needle and power supply read the same as an ammeter connected directly to the plate where charge neutralization occurred. This experiment was performed with high-conductivity solutions (10^{-4} – 10^{-3} M NaCl in methanol) at a flow rate of $8 \mu\text{L}/\text{min}$. If charge migration back toward the syringe pump were to occur, it would certainly be under these extreme conditions.

Stock solutions of NaCl (Columbus Chemical Industries, Columbus, WI) and tetrapentylammonium bromide ((TPA)Br, Aldrich Chemical Co., St. Louis, MO) were prepared in methanol (Burdick & Jackson, Muskegon, MI). Appropriate dilutions were then made from the stock. Conductance measurements were performed with a Barnstead (Boston, MA) model PM-70CB conductivity bridge and a YSI (Yellow Springs, OH) 3400 dip cell.

RESULTS AND DISCUSSION

Under Theory, we demonstrated that only in the case where iR_s is significant compared to V_{app} will the current–voltage curve for the overall ESI process differ significantly from that of the charge separation process alone. In the experiments discussed below, we have used a nonconducting needle in various configurations to observe the effect of iR_s under conditions where it could be significant.

Solution Resistance and Needle Geometry. In the first instance, it was desirable to change the solution resistance without changing the solution composition. This is to avoid the effect that a change in composition might have on the charge separation process. The solution resistance is related to the resistivity of the solution and the needle geometry by eq 4, where ρ is the resistivity

$$R_s = \rho \frac{L}{A} = \frac{1}{\kappa} \frac{L}{\pi r^2} = \frac{1.27}{\kappa} \frac{L}{d^2} \quad (4)$$

of the solution, κ is the solution conductivity, L is the length of the glass capillary comprising the needle, A is its inner cross-sectional area, r is the inner radius, and d is the inner diameter. A conductivity meter was used to measure the value of κ for each of the solutions used. From this measurement and the length and diameter of capillary used, the expected value for R_s could be calculated. These values, in terms of R_s per centimeter of capillary length, are shown in Table 1 for several solutions and several capillary diameters.

Needle Length. One of the factors affecting R_s in eq 4 is the length of the glass capillary needle. As the needle length decreases, R_s should decrease and the slope of the current–voltage curve (dI/dV) should increase. The dark data points in

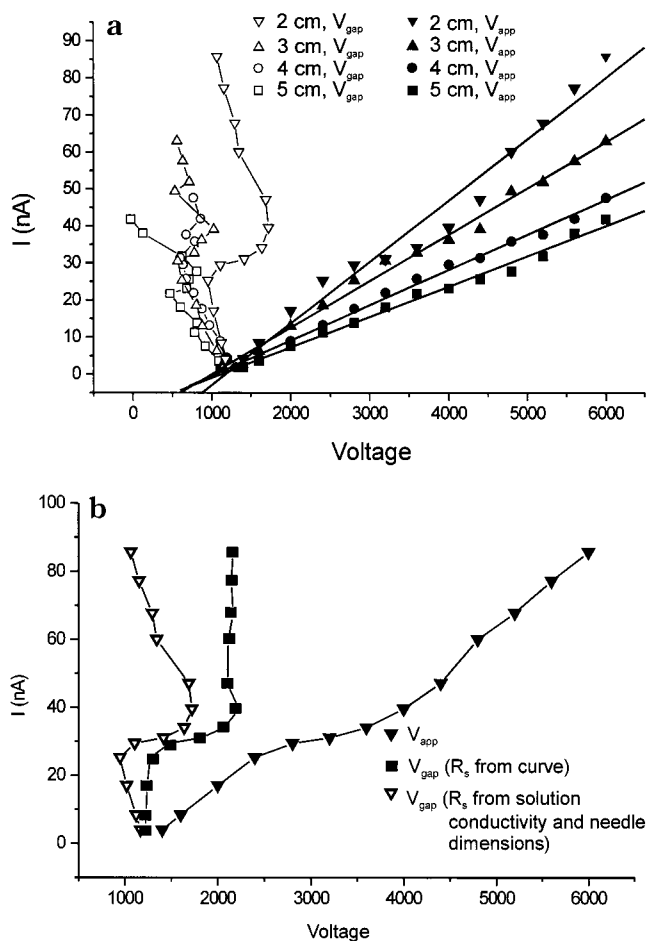


Figure 5. (a) Effect of glass needle length. The current vs V_{gap} and V_{app} is shown for 2, 3, 4, and 5 cm lengths of a $25 \mu\text{m}$ nonconducting glass capillary needle. The solution used contained 5×10^{-5} M TPA⁺ and 2×10^{-5} M Na⁺ in methanol. (b) Two different ways to determine V_{gap} . The current vs V_{gap} curve is shown for the case where R_s is determined from the current–voltage curve and the case where R_s is calculated from the measured solution conductivity and the glass needle dimensions.

Table 1

[TPABr], M, in methanol with 2×10^{-5} M NaCl	R_s , $\Omega \text{ cm}^{-1}$		
	$25 \mu\text{m}$ $\Omega \text{ cm}^{-1}$	$50 \mu\text{m}$ $\Omega \text{ cm}^{-1}$	$250 \mu\text{m}$ $\Omega \text{ cm}^{-1}$
0	4.06×10^{10}	1.02×10^{10}	4.06×10^8
5×10^{-6}	3.65×10^{10}	9.14×10^9	3.65×10^8
5×10^{-5}	2.88×10^{10}	7.20×10^9	2.88×10^8
5×10^{-4}	4.77×10^9	1.19×10^9	4.77×10^7

Figure 5a show this effect. The solution used contained 5×10^{-5} M TPA⁺ and 2×10^{-5} M Na⁺ in methanol. The nonconducting glass capillary needle was $25 \mu\text{m}$ in diameter. From the resistances in Table 1, we expect R_s to be $1.44 \times 10^{11} \Omega$ for the 5 cm needle, $1.15 \times 10^{11} \Omega$ for the 4 cm needle, $8.64 \times 10^{10} \Omega$ for the 3 cm needle, and $5.76 \times 10^{10} \Omega$ for the 2 cm needle. These values were used with eq 4 to calculate V_{gap} in Figure 5a. The plot of current vs V_{gap} essentially yields the current–voltage curve for the constant-current regulator generated by the needle tip, gap, and counter electrode. Unlike the case with the conducting needle where $V_{\text{gap}} = V_{\text{app}}$, V_{gap} is relatively constant for the nonconducting glass capillary needle. Thus, i (which is a measure of the rate of

excess charge production) for a given set of conditions is allowed to increase, while V_{gap} remains essentially the same.

Even though V_{gap} does not change nearly as dramatically as V_{app} , some structure is evident in the current vs V_{gap} curve. Some of this structure is due to the difference in the calculated resistance vs the actual resistance. For most of the analyses done in this paper, the solution resistances used to generate V_{gap} were calculated from conductivity measurements and glass capillary dimensions. This was done in order to unequivocally prove that the solution resistance was indeed the primary contributor to the resulting current–voltage curve. However, it should be possible to calculate an equivalent resistance from the slope of the i vs V_{app} curves in Figure 5a using eq 5. This empirically determined

$$\frac{1}{R} = \frac{di}{dV} = \text{slope} \quad (5)$$

resistance value would avoid errors due to imperfections in needle dimensions (a small error in capillary i.d. translates into a much larger error, since we are concerned with the area of the capillary hole), changes in room temperature (and thus conductivity), and any source of error associated with the device used as the conductivity meter. The results of this analysis are shown in Figure 5b. Note that the current vs V_{gap} curve that was obtained using R_s from the current–voltage curve necessarily has an infinite or positive slope (application of eq 5 automatically eliminates the negative slope). There is still some structure that is evident since V_{gap} increases by about 1 kV as it undergoes the transition from relatively low to relatively high current. This phenomenon will be seen in other current–voltage curves throughout this paper. Preliminary data from imaging indicate that a transition in ESI operating modes occurs in this region. This will be the topic of another paper. From these calculations and observations, we are confident that most of the slope in the linear regions of the current–voltage (V_{app}) curve in Figure 5a is due to the resistance of the solution.

Finally, to confirm that the current vs V_{app} curve does not change with needle length in the conducting needle, various lengths were used and the current–voltage curve was examined. The curves for the 6.8 and 3.0 cm lengths of metal needle were virtually identical.

Needle Diameter. Another factor that affects R_s according to eq 4 is the inner diameter of the glass capillary needle. As one would intuit from eq 4, the resistance of the solution decreases as the inner diameter of the needle increases. In fact, for the 25 and 50 μm glass spray needles, the values of R_s calculated from the current–voltage curve are always approximately 4 times larger for the 25 μm needle (for the same length and same solution) than one would expect from eq 4. This is shown in Figure 6. The solution used for this experiment was 2×10^{-5} M NaCl in methanol. Thus, from Table 1, the calculated solution resistances for the 25 and 50 μm needles (both were 5 cm long) are 2.03×10^{11} and $5.01 \times 10^{10} \Omega$. As before, these resistances calculated from the measured solution conductivity and the actual dimensions of the glass capillary were used to calculate V_{gap} . Again, V_{gap} is relatively constant under both sets of conditions. Finally, the R_s values calculated from the slope (see eq 5) of the experimentally generated current–voltage curves (2.31×10^{11} and $6.23 \times 10^{10} \Omega$) are once again in close agreement with those calculated using

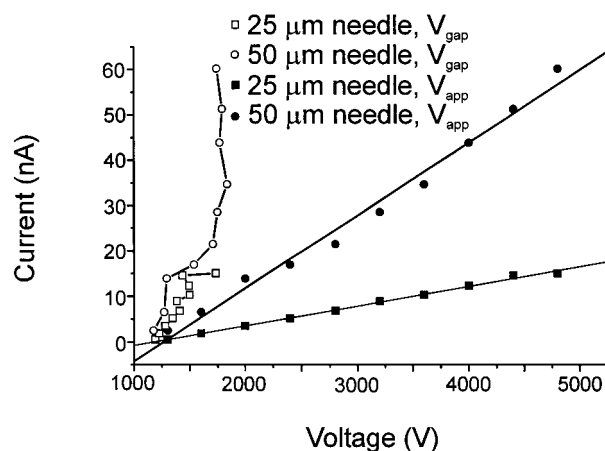


Figure 6. Effect of glass needle inner diameter. The current vs V_{gap} and V_{app} is shown for 25 and 50 μm inner diameter glass capillary spray needles. The solution used was 2×10^{-5} M NaCl in methanol.

the conductivity measurements and the dimensions of the glass capillary spray needle.

Solution Conductivity. The effect of solution conductivity has already been carefully characterized in the case of the metal spray needle. In general, the current, i , should be proportional to the conductivity of the solution, κ^n , where n has been determined to be a value in the range 0.22–0.57.^{18,19,23}

On the basis of the observations made above, a much more straightforward relationship is expected with the glass capillary spray needle. The slope of the current–voltage curve is determined by R_s when R_s is of appropriate magnitude. Thus, the slope of the current–voltage curve should change proportionally with the measured conductivity. The solutions in Table 1 were used with a 5 cm long, 25 μm glass spray needle. We expect the following ratios of the slopes for the current–voltage curves using the values from the conductivity meter in Table 1: 5×10^{-5} MTPA⁺/5 $\times 10^{-6}$ MTPA⁺ = 1.45 and 5×10^{-4} MTPA⁺/5 $\times 10^{-5}$ MTPA⁺ = 5.88 (all samples contain 2×10^{-5} M NaCl). The ratios from the plots of the current–voltage curves are 1.27 and 4.28, respectively. The differences in these ratios could be from errors associated with the conductivity meter, temperature differences in the laboratory on the day the two experiments were conducted, or dilution errors (since the measurements were conducted with two different sets of dilutions). However, the ratios measured from the ESI-generated current–voltage curve and from the conductivity meter are in close agreement. From this, we see that, with small-bore glass capillary needles, the current–voltage curve is dominated by the iR_s drop in the solution.

Glass Needle with a Series Resistor. We have hypothesized that the slope of the current–voltage curve is dictated by R_s when R_s is of appropriate magnitude. Therefore, if we put a resistor in series with the glass needle and power supply, the resulting slope should be consistent with the sum of the inserted resistance and the solution resistance. The results of this experiment for a methanol solution that contained 5×10^{-4} M TPA⁺ and 2×10^{-5} M Na⁺ in a 5 cm long, 25 μm needle with and without a $5 \times 10^{10} \Omega$ resistor in series are shown in Figure 7. The expected R_s without the resistor, as calculated from the values in Table 1, is $2.50 \times 10^{10} \Omega$. When the $5 \times 10^{10} \Omega$ resistor is in series with the

(23) Fernandez de la Mora, J.; Locortales, I. G. *J. Fluid Mech.* **1994**, *243*, 561.

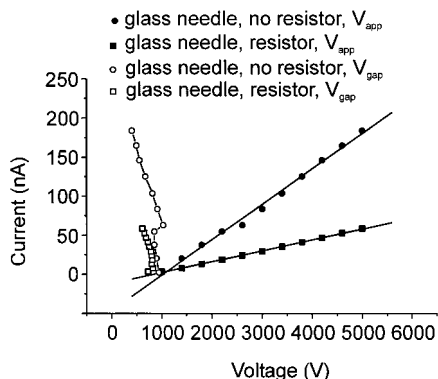


Figure 7. Effect of adding a large resistor ($5 \times 10^{10} \Omega$) in series with the glass spray needle.

glass needle, the expected resistance is $7.50 \times 10^{10} \Omega$. We used these values to calculate V_{gap} . In both instances, V_{gap} changes by about 400 V while V_{app} changes by 5 kV. Furthermore, the calculated total resistance from the slope of both current–voltage curves is in very close agreement with the expected values. Without the resistor, the R_s obtained from the slope of the curve is $2.21 \times 10^{10} \Omega$, and with the resistor, the overall resistance from the slope of the curve is $7.20 \times 10^{10} \Omega$.

We have pointed out that under the conditions that are usually observed in ESI, a resistor should be on the order of $10^{10} \Omega$ or larger to have a significant impact on the ESI circuit. However, in the case of the $250 \mu\text{m}$ glass capillary needle, the R_s is too small. This is shown in Figure 8a for a methanol solution that contains $5 \times 10^{-6} \text{ M TPA}^+$ and $2 \times 10^{-5} \text{ M Na}^+$ in a $250 \mu\text{m}$ glass needle with a length of 5 cm. The large diameter of the glass capillary results in a value for R_s considerably less than $10^{10} \Omega$. If we use the values in Table 1, the calculated R_s for this configuration is $1.83 \times 10^9 \Omega$. The resulting current–voltage curve now more resembles that of the metal needle. However, when the $5 \times 10^{10} \Omega$ resistor is put in series with the $250 \mu\text{m}$ glass spray needle, the total resistance is large enough to dictate the shape of the current–voltage curve (see Figure 8b). When V_{gap} is calculated using the $5 \times 10^{10} \Omega$ resistor, it remains essentially constant while the measured current for the ESI process changes by almost an order of magnitude. Here the current–voltage curve of the small-bore glass capillary (nearly constant V_{gap}) has been achieved by adding a series resistor.

Metal Needle with a Series Resistor. From previous observations and interpretations, it follows that a resistor placed in series with the metal spray needle should cause it to behave more like the glass spray needle. To test this hypothesis, the $5 \times 10^{10} \Omega$ resistor was placed in series with a metal spray needle. Figure 9 shows the current–voltage curves for $5 \times 10^{-6} \text{ M TPA}^+$ in a methanol solution. Note the increased operating range of the metal spray needle. At a distance of only 2.5 mm from the metal plate, no arcing occurs and no deviation from a stable Taylor cone is observed for a wide range of applied voltage (up to 6 kV). Furthermore, with the resistor in series with the metal spray needle, V_{gap} remains relatively independent of V_{app} and i . Also, the calculated resistance from the experimentally generated current–voltage curve is $5.2 \times 10^{10} \Omega$, well within the 10% tolerance of the resistor. This also underscores the point in the theory section that nothing in the circuit diagram for ESI with

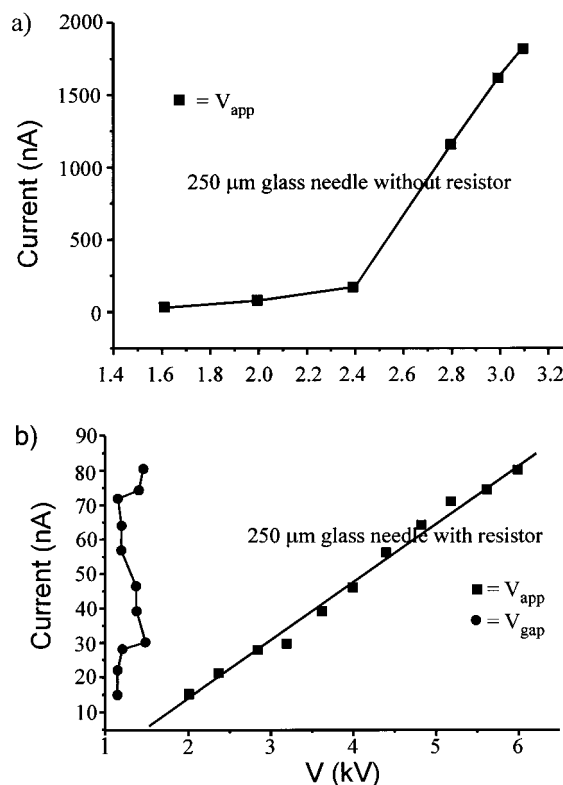


Figure 8. (a) Current–voltage curves for the $250 \mu\text{m}$ glass spray needle with no resistor and (b) the current vs V_{app} and V_{gap} for the $250 \mu\text{m}$ glass spray needle with a $5 \times 10^{10} \Omega$ resistor in series with the power supply.

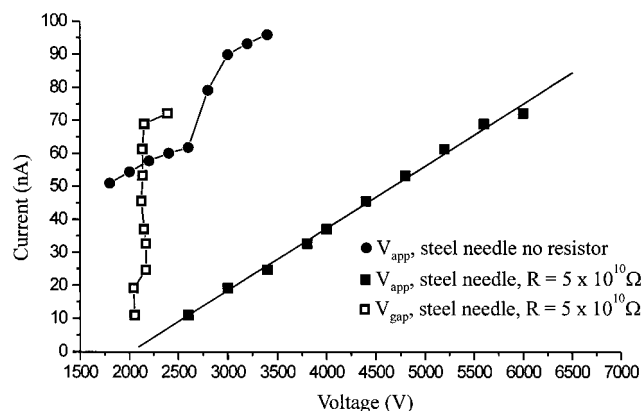


Figure 9. In the case of the metal needle, the current vs V_{app} and V_{gap} with a $5 \times 10^{10} \Omega$ resistor in series with the power supply and the current vs V_{app} (experimentally determined without any resistor).

the metal needle functions as a resistor, since all of the measured resistance can be attributed to the resistor that was put in series with the power supply. The similar operating characteristics of the nonconducting glass spray needle and the metal needle with the resistor lend justification to the claim that the unique behavioral characteristics of the nonconducting glass capillary are due to the resistance of the solution.

Also in Figure 9, the current–voltage curve for the metal needle without the resistor is shown and compared to the current–voltage curve for the metal needle with the resistor when the plotted voltage is V_{gap} . This plot in effect shows the current–voltage curve for the constant-current regulator generated by the spray needle tip, gap, and counter electrode with and without the

large resistor. In the case without the resistor, the current does increase with V_{app} (without the resistor $V_{\text{app}} = V_{\text{gap}}$), since the increase in field strength increases the rate of charge separation. Above 3.4 kV, a precipitous rise in current occurs with the onset of arcing. As already mentioned, this is analogous to the breakdown of the medium between the electrodes in a current-limited device. The gap voltage remains relatively constant when the large resistor is placed in series with the ESI power supply. Therefore, the current–voltage curves for these two cases look very different. Thus, it would appear that, yet again, the ESI process behaves very differently when an iR drop exists that is a significant fraction of V_{app} .

CONCLUSIONS

The dramatic effect of a significant iR drop on the current–voltage curve for the charge separation process in ESI has been conclusively demonstrated. The experimental situation will determine whether a significant iR drop exists. For example, a metal-coated glass spray needle^{24–27} would exhibit current–voltage characteristics that are similar to those of the metal spray needle. Indeed, current–voltage curves generated by Kriger et al.²⁶ with a gold-coated 25 μm glass capillary show a relatively flat region attributed to the constant-current regulator and the onset of arcing coupled with a dramatic rise in current at high V_{app} . Like the metal spray needle, the electrical connection is made directly to the needle where the spray occurs, so R_s is negligible. This same logic would hold for the case where the electrical connection is made

to the solution by a wire that is inserted into the glass capillary.^{28,29} If the wire is near enough to the needle tip, R_s will be negligible and will have minimal impact on the current–voltage curve. However, if the wire is pulled back far from the needle tip, R_s will become significant and will be proportional to the distance from the end of the wire and spray aperture of the glass capillary. In the particular case of Wang and Hackett,²⁸ a grounded conductive sheath was added to the outside of the capillary through which the internal wire connection was made. An additional length of a 20 μm glass capillary exit line was used between this connection region and the tip for low-flow-rate experiments. If charge separation is occurring in the connection region as a result of the capacitance between the outer sheath and inner connector, there will be a measurable current through the wire connecting the sheath to the ground. In any case, we agree with König and Fales³⁰ that a large-gap voltage exists ($V_{\text{app}} - iR_s$) and that the beneficial effects of the apparatus are due in large part to the solution resistance of the exit line.

ACKNOWLEDGMENT

We gratefully acknowledge the National Institutes of Health (Grant GM 49922) and Pfizer, Inc., for partial support of this work and Dr. Alan G. Marshall and Dr. Mark Emmett of the FT-ICR/MS group at the National High Magnetic Field Laboratory (NHMFL) for their tutorials in using the nonconducting glass needle. We also thank Mike Davenport for assistance with the instrumental electronics and Mike Davenport, Hoshang Shahvar, Terri L. Constantopoulos, and Nadja Lindley for helpful discussions.

Received for review February 25, 1999. Accepted May 17, 1999.

AC9902244

- (24) Valaskovic, G. J.; McLafferty, F. W. *J. Am. Soc. Mass Spectrom.* **1996**, *7*, 1270–1272.
- (25) Valaskovic, G. A.; Kelleher, N. L.; Little, D. P.; Aaserud, D. J.; McLafferty, F. W. *Anal. Chem.* **1995**, *67*, 3802–3805.
- (26) Kriger, S. M.; Ramsey, R. S.; Cook, K. D. *Anal. Chem.* **1995**, *67*, 385–389.
- (27) Wilm, M.; Mann, M. *Anal. Chem.* **1996**, *68*, 1–8.
- (28) Wang, H.; Hackett, M. *Anal. Chem.* **1998**, *70*, 205–212.
- (29) Fong, K. W. Y.; Dominic Chan, T.-W. *J. Am. Soc. Mass Spectrom.* **1999**, *10*, 72–75.
- (30) König, S.; Haegeler, K. D.; Fales, H. *Anal. Chem.* **1998**, *70*, 4453–4455.